ELSEVIER

Journal of Luminescence 81 (1999) 127–134

JOURNAL OF LUMINESCENCE

Free-induction fluorescence from Frenkel excitons in one-dimensional systems with substitutional traps: Effects of long-range interactions

V.A. Malyshev[a], A. Rodríguez[b], F. Domínguez-Adame[c,*]

[a] *All-Russian Research Center, "Vavilov State Optical Institute", Birzhevaya Liniya 12, 199034 Saint-Petersburg, Russian Federation*
[b] *GISC, Departamento de Matermática Aplicada y Estadística, Universidad Politécnica, E-20840 Madrid, Spain*
[c] *GISC, Departamento de Física de Materiales, Universidad Complutense, E-20840 Madrid, Spain*

Received 26 May 1998; received in revised form 1 October 1998; accepted 1 October 1998

Abstract

We study the effect of long-range interactions on the free-induction fluorescence from Frenkel excitons following after excitation by an ultrashort pulse of a small area. A non-perturbative contribution of far neighbors to the free-induction decay is found. The effect results from the non-perturbative renormalization of that part of the exciton energy spectrum (in the vicinity of the bottom of the excitonic band), which mainly contribute to the free-induction signal. We also analyze the applicability of the segment model to the problem of interest when including the coupling to far neighbors.

PACS: 71.35.Aa; 36.20.Kd; 78.30.Ly

Keywords: Frenkel excitons; Exciton trapping; Free induction fluorescence

1. Introduction

The model of Frenkel excitons in one-dimensional disordered lattices has been proven to be very useful in order to explain the low-temperature transport properties and photophysics of molecular aggregates [1] (see also the reviews [2,3] and references therein), polymer chains [4–9] as well as several antiferromagnets [10–12]. The latter systems present strong anisotropy in the hopping integrals for three crystallographic directions. One of the integrals is typically several orders of magnitude larger than the others and, consequently, the system can be treated within the quasi-one-dimensional approach.

Dynamics of one-dimensional Frenkel excitons is strongly affected by the disorder of different types. Fluctuations of both hopping integrals and site energies result in the localization of the exciton states, which is also reflected in the exciton optical dynamics. A great deal of work has been devoted to such problems during the last two decades (see the reviews [2,3]). In this paper we mainly focus our attention on the disorder produced by the presence of ions substituting host atoms. Such ions are randomly distributed in the host chain and can act in

* Corresponding author. Tel.: 3491 3944488; fax: 3491 3944547; e-mail: adame@valbuena.fis.ucm.es.

0022-2313/99/$ – see front matter
PII: S0022-2313(98)00154-9

a twofold way, first, localizing the excitons, and second, trapping them. Both effects have different manifestation in the exciton optical dynamics [8–11,13,14]. The authors of all just referred papers used the nearest-neighbor (NN) approximation in order to describe the exciton optical dynamics, assuming that coupling to far neighbors is negligible. However, previous works have shown that the inclusion of the long-range interactions strongly affects Frenkel exciton states in one-dimensional systems with continuous diagonal or off-diagonal disorder [15,16]. The main goal of the present papers is to show that the contribution of far neighbors to the linear optical response of one-dimensional Frenkel excitons cannot be perturbative. The reason of this effect becomes clear from the fact that the major contribution to the linear optical response is determined by the states of the bottom of the exciton band. The energies of these states undergo non-perturbative changes with inclusion of the coupling to far neighbors [17].

The remainder of the paper is organized as follows. In Section 2 we describe our model Hamiltonian and the way to calculate the free-induction fluorescence from Frenkel excitons under the condition of a short pulse excitation. In Section 3 we present the results of the nearest-neighbor approximation as applied to the case of low temperatures. Section 4 deals with the analytical treatment of the effect caused by the coupling to far neighbors. Section 5 is devoted to results of numerical simulations and discussions. As a main point, we will show that the long-range dipole–dipole interaction leads to a much faster fluorescence decay as compared to the nearest-neighbor interaction. Section 6 concludes the paper with a brief summary of results and some general remarks on their physical implications.

2. Model and basic relationships

We assume that a quencher substitutes a host atom, in such a way that the whole chain consists of a number of segments separated by quenchers (the so-called model of *disruptive* quenchers, according to the terminology proposed in Refs. [4]). The probability $p(N)$ to find a segment of N host atoms is $p(N) = c(1-c)^{N-1}$. At large N, which is of interest in most experimental situations, this quantity reduces to the Poissonian distribution $p(N) = c\exp(-cN)$.

In the model with only nearest-neighbor interactions between the host atoms, the problem of the optical response of the whole chain can be reduced to that for a segment with traps at either end. The result must then be averaged over the segment length distribution $p(N)$. On the one hand, inclusion of the coupling between far neighbors makes the segments dependent from each other and, on the other hand, renormalizes the exciton spectrum of each segment. The tight-binding Hamiltonian of the whole chain with all interactions reads

$$\begin{aligned}\mathscr{H} = &\sum_{n,m(m\neq n)} U_{mn} a_m^\dagger a_n - \sum_n \xi_n [U_{n-1,n}(a_n^\dagger a_{n-1} \\ &+ a_{n-1}^\dagger a_n) + U_{n,n+1}(a_n^\dagger a_{n+1} + a_{n+1}^\dagger a_n) \\ &+ \mathrm{i}\Gamma(a_{n-1}^\dagger a_{n-1} + a_{n+1}^\dagger a_{n+1})], \end{aligned} \tag{1}$$

where $a_n^\dagger$ (a_n) creates (annihilates) an exciton at site n and $U_{mn} = -U/|m-n|^3$ ($U>0$) is the dipole–dipole hopping integral. The stochastic variable ξ_n takes the values 1 and 0 with probability c and $1-c$, respectively. Here Γ is the quenching constant. We will only account for quenching in those host atoms which are nearest to traps. All the site energies are set to zero since we do not take into account any on-site disorder.

As it was established in Refs. [13,18], the optical response of the excitonic system to the action of an ultrashort pulse of small area consists of two components of emission, namely incoherent and coherent. The incoherent part describes the decay of the exciton population due to trapping. It is determined by the expectation value of the exciton number operator $\hat{n} = \sum_j a_j^\dagger a_j$, which is proportional to the Q-function introduced by Huber and Ching [13]. This part of emission will not be considered in the present work.

The coherent component, which we will be interested in, is associated with the expectation value of the dipole operator of the system with $\mathscr{N}$ sites

$$\bar{D}(t) = \mathrm{i}\frac{\theta}{\mathscr{N}}\langle 0|D\mathrm{e}^{-\mathrm{i}\mathscr{H}t}D|0\rangle, \tag{2}$$

where

$$D = \sum_{n=1}^{\mathcal{N}} (a_n^\dagger + a_n) \tag{3}$$

is the dipole operator of the whole chain (for the sake of simplicity, hereafter we substitute all the transition dipole matrix elements by unity and assume that the whole chain has a length less than the emission wavelength) and $|0\rangle$ denotes the ground state of the system. The evolution in time of the mean dipole is responsible for the free induction fluorescence emitted from the system. Its intensity is proportional to the square of the second derivative of $\bar{D}(t)$ averaged over an oscillation period and is linked with the P-function introduced in Ref. [13]

$$P(t) = \frac{1}{\mathcal{N}^2} |\langle 0|D e^{-i\mathscr{H}t} D|0\rangle|^2. \tag{4}$$

This equation is the basis of our analysis of the effects of long-range interactions on the decay of the excitonic free-induction fluorescence.

3. Nearest-neighbor approximation

To make clear the gist of the effects we are going to treat, let us turn first to the NN approximation. As it was mentioned above, one may then consider the segments to be independent of each other, owing to the presence of traps. It is obvious that under these conditions, both the Hamiltonian $\mathscr{H}$ and the dipole operator D split into a sum of independent blocks

$$\mathscr{H} = \sum_{\{N\}} \mathscr{H}_N, \tag{5a}$$

$$\mathscr{H}_N = -U \sum_{n=1}^{N} (a_n^\dagger a_{n+1} + a_{n+1}^\dagger a_n) - i\Gamma(a_1^\dagger a_1 + a_N^\dagger a_N), \tag{5b}$$

$$D = \sum_{\{N\}} D_N, \tag{5c}$$

$$D_N = \sum_{n=1}^{N} (a_n^\dagger + a_n), \tag{5d}$$

where the symbol $\sum_{\{N\}}$ means the summation over a stochastic realization of segments. The operators $\mathscr{H}_N$ and D_N are, respectively, the Hamiltonian and the dipole operator of a segment of size N, spanned on the corresponding subspace of eigenfunctions. Taking into consideration such a representation and assuming that the number of segments is large enough to treat $P(t)$ as a self-averaging quantity, one can rewrite Eq. (4) in the form

$$P(t) = \left| \frac{1}{\mathcal{N}} \sum_{\{N\}} \bar{D}_N(t) \right|^2 = \left| c \sum_N p(N) \bar{D}_N(t) \right|^2, \tag{6a}$$

$$\bar{D}_N(t) = \langle 0|D_N e^{-i\mathscr{H}_N t} D_N|0\rangle, \tag{6b}$$

where $p(N) = c(1-c)^{N-1}$ has the meaning defined above.

Note that Eq. (6a) differs from the analogous one used in previous studies [4,5,10], $P(t) = \sum_N p(N) |\bar{D}_N(t)|^2$. The latter implicitly assumed that there is no relative phase coherence in the radiation emitted by the individual segments so that the intensities of the radiation fields from the segments are added rather than the amplitudes as it takes place in Eq. (6a). In our opinion, such an assumption can be only justified at high temperatures when the relative phase coherence of segments can be destroyed due to the exciton–phonon interaction before the emission process starts. On the contrary, Eq. (6a) seems to be applicable at low temperatures. We will compare both coherent and incoherent approaches later.

There are two reasons for $P(t)$ to decay with time. The first one is naturally the presence of traps, while the second exists even in the absence of the trapping process. Indeed, using the completeness of the excitonic eigenstates $|k\rangle$ (related to a segment of length N), one can rewrite Eq. (6b) in the form

$$\bar{D}_N(t) = \sum_{k=1}^{N} |\langle 0|D_N|k\rangle|^2 e^{-iE_k(N)t}, \tag{7}$$

where $E_k(N)$ are the excitonic eigenenergies calculated for the segment of length N

$$E_k(N) = -2U \cos\frac{\pi k}{N+1}, \quad k = 1, 2, \ldots, N, \tag{8}$$

and $|\langle 0|D_N|k\rangle|^2$ is given by the expression

$$|\langle 0|D_N|k\rangle|^2 = \frac{1}{N+1}[1-(-1)^k]\cot^2\frac{\pi k}{2(N+1)}. \quad (9)$$

From Eq. (7) it follows that the magnitude $\bar{D}_N(t)$ is a finite linear combination of periodic functions of non-multiple frequencies. Therefore, the evolution in time of $\bar{D}_N(t)$ represents beatings, with no decay. Nevertheless, as the frequencies of components fluctuate, the averaged contribution of each one and, as a result, $P(t)$ will decrease in time, owing to the destructive interference of oscillations with continuously distributed frequencies. Our main goal now is to discuss the latter mechanism of decay of the free induction fluorescence, neglecting the traps in the Hamiltonian (5b) for a moment.

Let us assume further that $c \ll 1$, which means that typically one has $N \gg 1$. In this case, $|\langle 0|D_N|k\rangle|^2 \approx 8N/(\pi k)^2$, with $k = 1, 3, 5, \ldots$. One can also use in Eq. (7) an approximate expression for the exciton energies, $E_k(N) = -2U + U(\pi k)^2/N^2$, and substitute $p(N)$ in Eq. (6a) by the Poisson law. Due to the steep decrease of $|\langle 0|D_N|k\rangle|^2$ with k, the main contribution to $P(t)$ comes obviously from the lowest excitonic state (with $k = 1$). This allows us to limit the summation over k in Eq. (7) by only the first term. Thus, finally we will get

$$P(t) = \left(\frac{8}{\pi^2}\right)^2 \left| c^2 \sum_N \mathrm{e}^{-cN} N \exp\left(-\mathrm{i}\frac{\pi^2 Ut}{N^2}\right)\right|^2. \quad (10)$$

Passing in Eq. (10) from the summation over N to the integration, Eq. (6a) will read

$$P(t) = \left(\frac{8}{\pi^2}\right)^2 \left| \int_c^\infty \mathrm{d}\xi\, \mathrm{e}^{-\xi}\xi \exp\left(-\mathrm{i}\frac{\pi^2 c^2 Ut}{\xi^2}\right)\right|^2. \quad (11)$$

The factor $\exp(-\xi)$ approximately restricts the region of integration to $\xi \leqslant 1$. On the other hand, the interval $\xi < \pi c(Ut)^{1/2}$ does not contribute to the integral in Eq. (11) due to fast oscillations of the temporal exponent. As the size of this interval grows with time, the magnitude of integral will decrease and approach zero at $\pi^2 c^2 Ut > 1$. It is a matter of simple calculations to show from Eq. (11) that the decay is quadratic for very short times ($\pi^2 Ut \ll 1$): $P(t) = (8/\pi^2)^2[1 - (\frac{1}{2})(\pi^2 cUt)^2]$, whereas the decay is linear for larger times ($c^{-2} > \pi^2 Ut \gg 1$): $P(t) = (8/\pi^2)^2[1 - (\frac{1}{2})\pi^3 c^2 Ut]$. In the latter case, one can replace the lower limit of integration by zero.

4. All interactions

There are at least two reasons for $P(t)$ to be renormalized with including all interaction as compared to the NN approach. First, the representation of the whole chain as a number of independent segments here is no longer valid since neighboring segments are coupled to each other by the dipole–dipole interactions of the next neighbors. Second, even if we neglect this coupling, non-perturbative effect arises from renormalization of the eigenenergies of each segment, as we will see below.

4.1. Effect of segment coupling

In order to gain insight into the problem of segment coupling, let us turn to the simplest case assuming that (i) the chain has only one trap, which divides it into two segments of sizes $N \gg 1$ and $M \gg 1$, (ii) the exciton problem of each isolated segment is treated in the NN approximation, (iii) the segments are coupled by the dipole–dipole interaction of sites being nearest to the trap, (iv) the trapping itself is neglected. The Hamiltonian of such a problem reads

$$\mathscr{H} = \mathscr{H}_N + \mathscr{H}_M + V, \quad (12)$$

where the Hamiltonians of the isolated segments are

$$\mathscr{H}_N = -U\sum_{n=1}^{N}(a_n^\dagger a_{n+1} + a_{n+1}^\dagger a_n), \quad (13a)$$

$$\mathscr{H}_M = -U\sum_{m=1}^{m}(b_m^\dagger b_{m+1} + b_{m+1}^\dagger b_m), \quad (13b)$$

where the operators $a_n, a_n^\dagger$ and $b_m, b_m^\dagger$ are related to the segments with N and M sites, respectively, and the interaction Hamiltonian reads

$$V = -\frac{U}{8}(a_N^\dagger b_1 + b_1^\dagger a_N). \quad (14)$$

Under these conditions, we aim to elucidate whether the interaction Hamiltonian V can be considered as a perturbation. Making use of the

excitonic transformations of the site operators a_n and b_m

$$a_n = \left(\frac{2}{N+1}\right)^{1/2} \sum_{k=1}^{N} \alpha_k \sin\frac{\pi k n}{N+1}, \tag{15a}$$

$$b_m = \left(\frac{2}{M+1}\right)^{1/2} \sum_{k=1}^{m} \beta_k \sin\frac{\pi k m}{M+1}, \tag{15b}$$

the different terms of the Hamiltonian (12) become

$$\mathscr{H}_N = \sum_{k=1}^{N} E_k(N)\,\alpha_k^{\dagger}\alpha_k, \quad E_k(N) = -2U\cos\frac{\pi k}{N+1}, \tag{16a}$$

$$\mathscr{H}_M = \sum_{k=1}^{m} E_k(M)\,\beta_k^{\dagger}\beta_k, \quad E_k(M) = -2U\cos\frac{\pi k}{M+1}, \tag{16b}$$

$$V = \sum_{k=1}^{N}\sum_{k'=1}^{m} V_{kk'}(\alpha_k^{\dagger}\beta_{k'} + \beta_{k'}^{\dagger}\alpha_k), \tag{16c}$$

where

$$V_{kk'} = \frac{(-1)^k U}{4\,(N+1)^{1/2}(M+1)^{1/2}} \sin\frac{\pi k}{N+1}\sin\frac{\pi k'}{M+1}. \tag{17}$$

As the interaction Hamiltonian couples the exciton states of one segment, $|k,N\rangle$, to those of the other one, $|k',M\rangle$, we should compare the energy differences $\Delta E_{kk'} = 2U|\cos[\pi k/(N+1)] - \cos[\pi k'/(M+1)]|$ with the magnitudes of $V_{kk'}$. At the region of interest ($k \ll N+1$, $k' \ll M+1$), one has

$$\left|\frac{V_{kk'}}{\Delta E_{kk'}}\right| = \frac{(N+1)^{1/2}(M+1)^{1/2}}{4|N-M|(N+M+2)}kk'. \tag{18}$$

Accounting for the fact that only values of $k = k' = 1$ actually contribute to the exciton free induction fluorescence, from Eq. (18) it follows that $|V_{kk'}| < |\Delta_{kk'}|$, excluding the low probable event $N = M$. Thus, the segment coupling through the far neighbors can be neglected in average and, subsequently, the segments themselves can be considered as independent one from another.

This result can appear somewhat counterintuitive. In principle, one would expect that the larger the segments, the closer their energies, which, in turn, would imply stronger interaction, in contrast to what is found in Eq. (18). However, a more careful consideration of this puzzling result allows to unconver its explanation: The key fact is that the probability amplitude of finding an exciton on the nearest site to the trap is given by $[2/(N+1)]^{1/2}\sin[\pi k/(N+1)]$, which is of the order of $(N+1)^{-3/2}$ for $k = 1$ as the segment size N increases. This effectively decouples the segments, thus counteracting the opposite tendency (indeed, as we have seen, prevailing over it) due to the above-mentioned energetic approaching.

4.2. Effect of renormalization of the energy spectrum

Now, let us turn to the effect of the eigenenergy renormalization on the exciton free induction signal. We will exploit the fact that the characteristic time of the free induction decay is determined by the energy of the lowest excitonic levels. In consistence with the results obtained in Ref. [17], just over this region the excitonic spectrum is noticeably renormalized with including all interactions, taking the form ($N \gg 1$)

$$E_k(N) = -2U\xi(3) + UK^2\left(\tfrac{3}{2} - \ln K\right),$$

$$K = \frac{\pi k}{N}, \quad k = 1, 2, \ldots, k \ll N, \tag{19}$$

where $\xi(3) = \sum_n n^{-3} = 1.202$. On the other hand, as it was established in Ref. [17], the exciton eigenfunctions are not changed, in fact, with including all dipolar interactions. Thus, we do not expect any influence of this type of renormalization on the signal of the free induction fluorescence. Consequently, we can approximate the matrix element $|\langle 0|D_N|k=1\rangle|^2$ by $(8/\pi^2)N$, as we have already done to arrive at Eqs. (10) and (11).

Accounting for the facts just mentioned, we finally obtain

$$P(t) = \left(\frac{8}{\pi^2}\right)^2 \left|\int_c^{\infty} \mathrm{d}\xi\, \mathrm{e}^{-\xi}\xi \times \exp\left[-\mathrm{i}\frac{\pi^2 c^2 U t}{\xi^2}\left(\frac{3}{2} - \ln\frac{\pi c}{\xi}\right)\right]\right|^2, \tag{20}$$

instead of the expression (11). Now, the exciton free induction fluorescence will disappear when $\pi^2 c^2 U t[3/2 - \ln(\pi c)] > 1$. This inequality differs from the analogous one obtained in the

NN-approximation (see Section 3) by the factor in parenthesis. It can noticeably deviate of unity at low concentration of traps, giving rise, respectively, to a faster decay of the free induction signal.

5. Numerical results and discussions

In this section we present results of numerical simulations demonstrating the correctness of our different approximations and particularly the effects of the long-range dipolar coupling. In what follows, we will evaluate the free induction fluorescence intensity as a function of the dimensionless time $\pi^2 c^2 Ut$. Fig. 1 shows the free induction fluorescence signal in the NN approximation for different values of c according to Eq. (10) and the results from Eq. (11), as a function of the dimensionless time $\pi^2 c^2 Ut$. We notice that $P(t)$ converges towards a *universal* curve on decreasing c and this curve is given by Eq. (11). In fact, for lower values of c (not shown in the figure), the results from Eqs. (10) and (11) are superposed.

Up to now, we have neglected the effects of excitonic states with k greater than unity. The next state with an appreciable contribution to the free induction signal is that with $k = 3$. Its oscillator strength is reduced by a factor $\frac{1}{9}$ as compared to the oscillator strength of the ground exciton state, whereas its energy is $E_3(N) = -2U + 9\pi^2 U/N^2$. The free induction fluorescence in the limit $N \gg 1$ then becomes

$$P(t) = \left(\frac{8}{\pi^2}\right)^2 \left| \int_c^\infty d\xi\, e^{-\xi} \xi \left[\exp\left(-i \frac{\pi^2 c^2 Ut}{\xi^2} \right) + \frac{1}{9} \exp\left(-i \frac{9\pi^2 c^2 Ut}{\xi^2} \right) \right] \right|^2, \tag{21}$$

in the NN approximation. From Eq. (21) we obtain that $P(t) = (8/\pi^2)^2[1 - (\frac{9}{2})(\pi^2 cUt)^2]$ for $\pi^2 Ut \ll 1$ and $P(t) = (80/9\pi^2)^2\,[1 - (9/10)\pi^3 c^2 Ut]$ for $c^{-2} > \pi^2 Ut \gg 1$, so that the initial decay is faster than that obtained for $k = 1$. However, at longer times the contribution of $k = 3$ can be confidently neglected, as seen in Fig. 2, at least compared to far neighbor coupling effects (see below). Higher values of k produce even smaller corrections. Thus, we conclude that in the coherent approximation the decay of the free induction signal mainly arises from the destructive interference between the lowest excitonic modes ($k = 1$) belonging to different segments. It should be noticed that in the model with no phase

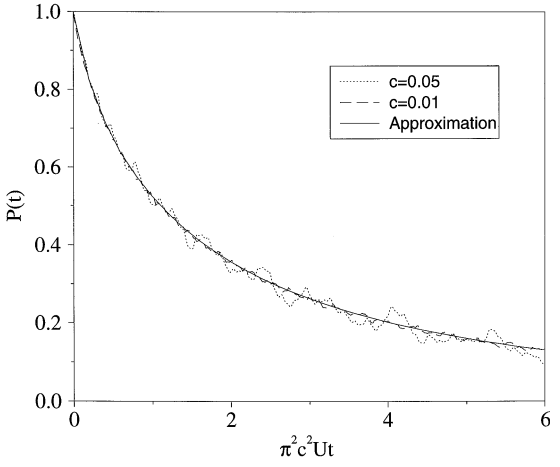

Fig. 1. Plots of the free induction fluorescence decay calculated using Eq. (10) for $c = 0.05$ (dashed line) and $c = 0.01$ (dotted line). Solid line shows the result obtained from Eq. (11). All curves are normalized to unity at $t = 0$.

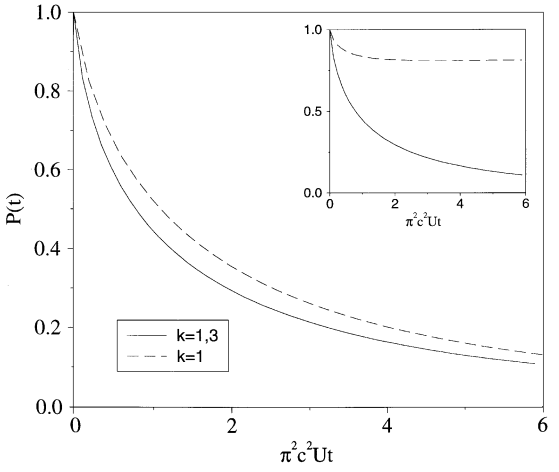

Fig. 2. Plots of the free induction fluorescence decay calculated using Eq. (11) (dashed line) and Eq. (21) (solid line). All curves are normalized to unity at $t = 0$. The inset compares the results for the coherent (solid line) and incoherent (dashed line) approximations for the two lowest exciton modes ($k = 1,3$).

coherence between segments [4,5,10] one obtains no decay when higher modes ($k > 1$) are neglected. Therefore, the next state with an appreciable oscillator strength ($k = 3$) should be taken into account. In such a case, the free induction fluorescence coming from each segment is proportional to $\frac{82}{81} + (\frac{2}{9})\cos[(E_3 - E_1)t]$. The average of this quantity results in a decaying signal as time elapses. Since the weight of $k = 3$ mode in the whole signal is $\frac{1}{9}$, one should expect a drop of the same order in the emission intensity from the initial value. The inset of Fig. 2 compares the results for the coherent $[P(t) \sim |\sum_N p(N)\bar{D}_N(t)|^2]$ and incoherent $[P(t) \sim \sum_N p(N)|\bar{D}_N(t)|^2]$ approximations for two lowest exciton modes ($k = 1, 3$), showing a dramatical difference between these two approximations and confirming our qualitative considerations.

According to Ref. [10], finite values of the quenching constant modifies the eigenenergy $E_1(N)$. In the limit $\Gamma \ll U$, which is of interest in most experiments, the perturbed eigenenergy is given by $\tilde{E}_1(N) = E_1(N) - 4i\pi^2\Gamma/N^3$ when $N \gg 1$. As the correction is of order N^{-1} as compared to the unperturbed eigenenergy, we cannot expect a significant contribution of finite values of the quenching constant for small c. In fact, this is the case for parameters of interest. Replacing $E_1(N)$ by $\tilde{E}_1(N)$ in Eq. (6a) and passing to integration we obtain

$$P(t) = \left(\frac{8}{\pi^2}\right)^2 \left| \int_c^\infty d\xi\, e^{-\xi}\xi \times \exp\left[-i\frac{\pi^2 c^2 U t}{\xi^2}\left(1 - i\frac{4c\Gamma}{U\xi}\right)\right]\right|^2. \quad (22)$$

Notice that the correction depends on $c\Gamma/U$, which is usually rather small in most physical systems since $\Gamma \ll U$ and $c \ll 1$. Fig. 3 shows that the decay curve obtained from Eq. (22) for small values of the parameter $c\Gamma/U$ is essentially the same as that obtained from Eq. (10). We observe deviations only for higher (and rather unphysical) values of that parameter. Thus we are led to the conclusion that the limit $\Gamma \to 0$ provides a fairly good description of the free induction fluorescence as far as the parameter $c\Gamma/U$ remains small.

Finally, let us now turn to the main aim of the paper, namely the effects of the dipolar coupling between far neighbors. From Eq. (20) it is clear that the free induction fluorescence does not converge towards a universal curve as a function of the dimensionless time on decreasing c, as it is seen in Fig. 4. We notice that there exists an appreciable deviation on the fluorescence decay curves when dipolar coupling is taken into account, as

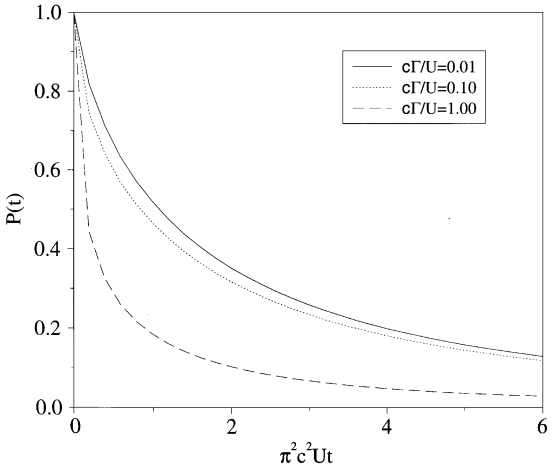

Fig. 3. Plots of the free induction fluorescence decay calculated using Eq. (22) with $c\Gamma/U = 0.01$ (solid line), 0.10 (dotted line) and 1.00 (dashed line). All curves are normalized to unity at $t = 0$.

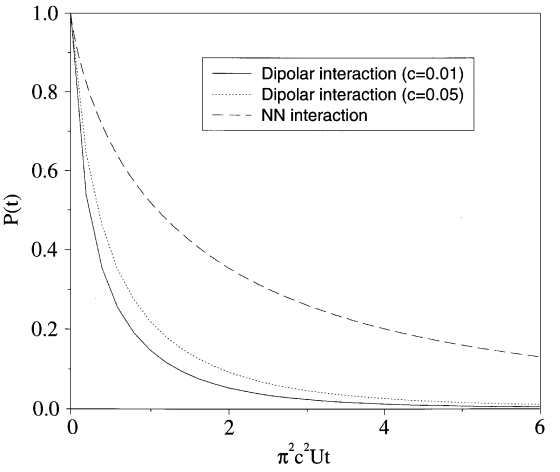

Fig. 4. Plots of the free induction fluorescence decay calculated using Eq. (20) for $c = 0.05$ (dotted line) and $c = 0.01$ (solid line). Dashed line shows the result obtained from Eq. (11). All curves are normalized to unity at $t = 0$.

compared to the NN approximation. This effect is higher on decreasing c, namely when the segment lengths are larger.

6. Conclusions

We have shown that the coupling to far neighbors substantially affects the decay rate of the free induction fluorescence from one-dimensional Frenkel excitons created by an ultrashort pulse of a small area in a chain with substitutional traps. Due to the non-perturbative nature of the effect, it must be accounted for at the fitting of the experimental data. Exciton trapping almost does not influence the free induction decay, excluding the case of very high concentration of traps. The free induction signal vanishes in time mainly due to fluctuations of the exciton energies of segments in which the whole chain is divided by the traps.

Acknowledgements

The authors gratefully thank D.L. Huber, R. Brito, A. Sánchez for numerous helpful conversations. Work at Russia has been supported by the Russian Foundation for Basic Research under Project No. 96-02-18292. Work at Madrid has been supported by CICYT (Spain) under Project No. MAT95-0325.

References

[1] E.W. Knapp, Chem. Phys. 85 (1984) 73.
[2] F.C. Spano, J. Knoester, in: W.S. Warren (Ed.), Advances in Magnetic and Optical Resonance, vol. 18, Academic Press, New York, 1994, p. 117.
[3] J. Knoester, F.C. Spano, in: T. Kobayashi (Ed.), J-aggregates, World Scientific, Singapore, 1996, p. 111.
[4] R.M. Pearlstein, J. Chem. Phys. 56 (1972) 2431.
[5] R.P. Hemeger, R.M. Pearlstein, Chem. Phys. 2 (1973) 424.
[6] R.P. Hemenger, K. Lakatos-Lindenberg, R.M. Pearlstein, J. Chem. Phys. 60 (1974) 3271.
[7] P.E. Parris, Phys. Rev. B 40 (1989) 4928.
[8] D.L. Huber, W.Y. Ching, Chem. Phys. 146 (1990) 409.
[9] Th. Wagersreiter, H.F. Kauffmann, Phys. Rev. B 50 (1994) 9102.
[10] D.L. Huber, Phys. Rev. B 45 (1992) 8947.
[11] X. Wu, W.M. Dennis, W.M. Yen, W. Jia, D.L. Huber, J. Lumin. 58 (1994) 361.
[12] V. Eremenko, V. Karachevtsev, V. Shapiro, V. Slavin, Phys. Rev. B 54 (1996) 447.
[13] D.L. Huber, W.J. Ching, Phys. Rev. B 42 (1990) 7718.
[14] F. Domínguez-Adame, B. Méndez, A. Sánchez, E. Maciá, Phys. Rev. B 49 (1994) 3839.
[15] H. Fidder, J. Knoester, D.A. Wiersma, J. Chem. Phys. 95 (1991) 7880.
[16] G.G. Kozlov, V.A. Malyshev, F. Domínguez-Adame, A. Rodríguez, Phys. Rev. B 58 (1998) 5367.
[17] V. Malyshev, P. Moreno, Phys. Rev. B 51 (1995) 14587.
[18] V.A. Malyshev, D.L. Huber, Phys. Rev. B 54 (1996) 8.